Chapter 36
Reduced-Order Modelling for Investigating Nonlinear FEM Systems

I. Tartaruga, S. A. Neild, T. L. Hill, and A. Cammarano

Abstract Modern finite element (FE) packages are capable of capturing nonlinear behaviour in extremely complex structures. However, due to the scale of these models, full dynamic analysis is often prohibitively expensive. An alternative approach is to use the FE models to derive reduced-order models (ROMs) which capture the dynamic behaviour of interest at a significantly lower computational cost. An automatic identification of the stated ROMs is powerful and desirable when parametric, sensitivity and uncertainty analysis is of interest. The authors implemented in Matlab a strategy to automatically compute the reduced order model and investigate the effects of parametric variation exchanging information with FEM software. In the strategy it is adopted the Applied Modal Force (AMF) approach, where a force is applied to the FE model and the resulting displacements are used to identify coefficients of the ROM, as is done in the ICE method. The developed techniques are presented in the paper and validated considering a crossed beam structure modelled in Abaqus.

Keywords Nonlinear dynamics · Reduced order model · Finite element model · Nonlinear normal mode · Parametric variation

Nomenclature

$[M]$	physical mass matrix
$[K]$	physical stiffness matrix
$[\Phi]$	matrix of eigenvector
$[\Phi_T]$	truncated $[\Phi]$
$\left[\overline{M}\right]$	modal mass matrix
$\left[\overline{K}\right]$	modal stiffness matrix
$\left[\overline{M}\right]_T$	truncated $\left[\overline{M}\right]$
$\left[\overline{K}\right]_T$	truncated $\left[\overline{K}\right]$
$\{x\}$	vector of physical coordinates
$\{q\}$	vector of modal coordinates
$\{q\}_T$	truncated $\{q\}$
$\{f_{nl}\}$	vector of physical generalized nonlinear forces
$\left\{\overline{f_{nl}}\right\}$	vector of modal generalized nonlinear forces
$\left\{\overline{f_{nl}}\right\}_T$	truncated $\left\{\overline{f_{nl}}\right\}$
$\{F\}$	vector of physical generalized linear forces
$\left\{\overline{F}\right\}$	vector of modal generalized linear forces
$\left\{\overline{F}\right\}_T$	truncated $\left\{\overline{F}\right\}$
R	number of retained modes in the reduction
Tol_m	tolerance adopted for retaining more modes

I. Tartaruga (✉)
Department of Engineering Mathematics, University of Bristol, Bristol, UK
e-mail: irene.tartaruga@bristol.ac.uk

S. A. Neild · T. L.Hill
Department of Mechanical Engineering, University of Bristol, Bristol, UK

A. Cammarano
School of Engineering, University of Glasgow, Glasgow, UK

G. Kerschen (ed.), *Nonlinear Dynamics, Volume 1*, Conference Proceedings of the Society for Experimental Mechanics Series, https://doi.org/10.1007/978-3-319-74280-9_36

Tol_f tolerance adopted for identifying the input set
$\{C\}_p$ vector of scale factors
t_R referential thickness
S_f scale factor adopted to rescale the input set
V_f scale factor adopted to rescale the input set
S scale factor

36.1 Introduction

The development of techniques able to investigate and deal with dynamic systems that exhibit nonlinearities has been of interest for academic researchers for decades. Recently, industrial interest has also been growing rapidly due to the desire to design lighter and hence more flexible structures [1, 2]. The industrial interest has pushed and motivated even more researchers to enhance already developed methodologies and conceive new strategies. Of particular interest is the possibility of dealing with nonlinearities in the real world; such an ambition requires a suitable modelling of the systems and phenomena of interest and an exchange of information between numerical and experimental analyses. The modelling needs to swit the aim of the research, which can require higher accuracy for specific aspects, such as stability analysis, coupling effects, modal interactions, resonances. The challenge in the analysis of nonlinearities is the often increased complexity in the modelling. In such a scenario, it is significant to identify and adopt techniques that are able to retain sufficient information from the real physics of a system/phenomena of interest reducing the degree of complexity allowing the investigation of nonlinear effects in a realistic time. Developing techniques able to reduce the complexity of a system, researchers have faced the problem of understanding what dynamics are to be retained for the system of interest, the limits and the effects of the assumptions and simplifications [3–7]. In the last two decades, reduced order modelling strategies, as well as identification techniques, have been widely considered in engineering fields to deal with nonlinearities in numerical and experimental systems, respectively [8–18]. In the development of reduced order models, Enforced Modal Displacement (EMD) and Applied Modal Force (AMF) techniques have been widely considered. To the best of the author's knowledge, the nonlinear reduced order model techniques still lacks robustness and automatization. The lack of robustness arises from the sensibility of the values of the coefficients adopted in reduced order models to the variation of the criteria adopted for the reduction. The criteria are in terms of: which set of static forces and modes to adopt for the reduction. The lack of automatization is due to the difficulty of performing uncertainty and sensitivity analysis. This paper will cover mainly progression in terms of automatization showing the effects of considering different modes. It presents the developed Matlab code that allows the application of EMD and AMF techniques. The developed code allows the interchange of information with finite element analysis (FEA) programs (such as Abaqus or Nastran) in an automatic environment, if either EMD or AMF technique is adopted. The code allows parametric studies and investigation of the effect of asymmetry. In the paper, a crossed beam modelled in Abaqus will be considered and the investigation of nonlinear behaviour will be done using backbone curves or nonlinear normal modes (NNM) [19], system characteristics recently adopted to investigate nonlinearities [2, 20–24].

36.2 Methodology

The techniques considered here are based on the reduced order model concept applied to FE model and have been implemented in Matlab. The most general equation for a FE model is the following

$$[M]\{\ddot{x}\} + [K]\{x\} + \{f_{nl}(x)\} = \{F\} \tag{36.1}$$

Where $[M]$, $[K]$, $\{\ddot{x}\}$, $\{x\}$, $\{f_{nl}(x)\}$ and $\{F\}$ are the matrices of inertia and stiffness, vector of generalised states-acceleration and states, vector of generalised nonlinear force and linear force.

For reduction purpose, Eq. 36.1 needs to be projected in a space where further information can be adopted by the user to reduce the order of the system of interest. The reduction is in terms of the degrees of freedom, acting forces and nonlinearities due to inherent characteristics of the system or interaction with the environment, external to the system itself. The EMD and the AMF project the equations in the linear modal space, this is accomplished using the matrix of linear eigenvectors $[\Phi]$ for the projection. The physical states are then projected and $x = [\Phi]\, q$; to complete the projection the Eq. 36.1 is premutliplied by $[\Phi]^T$. The two steps to project the physical space to the modal one are presented in Eq. 36.2

$$[\Phi]^T \left([M][\Phi]\{\ddot{q}\} + [K][\Phi]\{q\} + \{f_{nl}\}([\Phi]\{q\})\right) = [\Phi]^T\{F\}$$
$$\left[\overline{M}\right]\{\ddot{q}\} + \left[\overline{K}\right]\{q\} + \left\{\overline{f_{nl}}(\{q\})\right\} = \left\{\overline{F}\right\} \tag{36.2}$$

In Eq. 36.2, $\left[\overline{M}\right]$, $\left[\overline{K}\right]$ and $\left\{\overline{f_{nl}}\right\}$ are the modal mass and stiffness matrices and the nonlinear force vector projected in the modal space. $\{q\}$ is the vector of modal coordinates.

All the coefficients in Eq. 36.2 are known except the nonlinear one. In fact, the modal matrices can be derived from FEM software. At this point three main questions need to be answered to continue the reduction of the original physical systems:

1. how to describe the nonlinear modal force ($\left\{\overline{f_{nl}}\right\}$) in terms of the modal coordinates if the nonlinear force $\{f_{nl}(x)\}$ is not analytically known.
2. how many modes and which one to retain, i.e. how to truncate the modal projection.
3. how to define the analysis to be accomplished to identify coefficients characterizing the reduced order model

36.2.1 Nonlinear Modal Force

The first point, the description of the nonlinear modal force ($\left\{\overline{f_{nl}}\right\}$), is generally [1, 5, 7, 25] accomplished considering quadratic and cubic nonlinear terms as it follows

$$([\Phi]^T\{f_{nl}\}([\Phi]\{q\}))_m = \left(\left\{\overline{f_{nl}}\right\}(\{q\})\right)_m =$$
$$= \sum_i \sum_j \sum_k (A_{ijk})_m q_i q_j q_k + \sum_i \sum_j (B_{ij})_m q_i q_j \tag{36.3}$$

Where the indexes i, j, k and m refer to the modal coordinates whose number R is given by truncation, i.e. if R is the number of retained modes, then $i, j, k, m = 1 \ldots R$.

When dealing with FEM models that present geometric nonlinearities, the use of the quadratic and cubic terms is a sensible choice, as demonstrated [1, 18].

The coefficients A_{ijk} and B_{ij} need to be identified, the process for the identification is the key step that differentiates the Applied Modal Force (AMF) and Enforced Modal Displacement (EMD) techniques. Both the techniques adopt static responses, a set of static physical force (F) and static physical deformation (x) are adopted as input in the analysis if the AMF and EMD techniques are adopted, respectively. Figure 36.1 shows two flow charts describing how the identification of the coefficients A_{ijk} and B_{ij} in Eq. 36.3 is accomplished. The input set (in terms of force F or deformation x) is considered and the static response obtained (in terms of deformation x or force F). Then the truncation is accomplished, and the known modal and stiffness reduced matrices are obtained. Using the static input and responses the coefficients adopting in the description of the nonlinear terms can be also obtained; the least square methods together with constraints due to energy consideration [18] is used. The number of considered static responses need to be at least equal to the sum of the considered quadratic and cubic terms.

36.2.2 Truncation

A crucial point when a reduced order method is adopted is the selection of modes to be retained. Most of the time there is not a clear knowledge of the modes that significantly affect the responses of interest, such as stability analysis. Ideally, the modal participation characterizing the responses of interest should be adopted to identify the modes to be retained; unfortunately this is not easily available especially in the presence of numerical systems with many degrees of freedom and experimental systems. In the present application, the modes are selected iteratively without considering the actual solutions. This is because the main point we want to underline is that the efficiency of modal reduction techniques is dictated by the number of evaluations of the actual system of interest. Having selected the first set of modes, the truncated equations projected in the modal space is obtained (Eq. 36.4).

$$\left[\overline{M}\right]_T\{\ddot{q}\}_T + \left[\overline{K}\right]_T\{q\}_T + \left\{\overline{f_{nl}}\right\}(\{q\})_T = \left\{\overline{F}\right\}_T \tag{36.4}$$

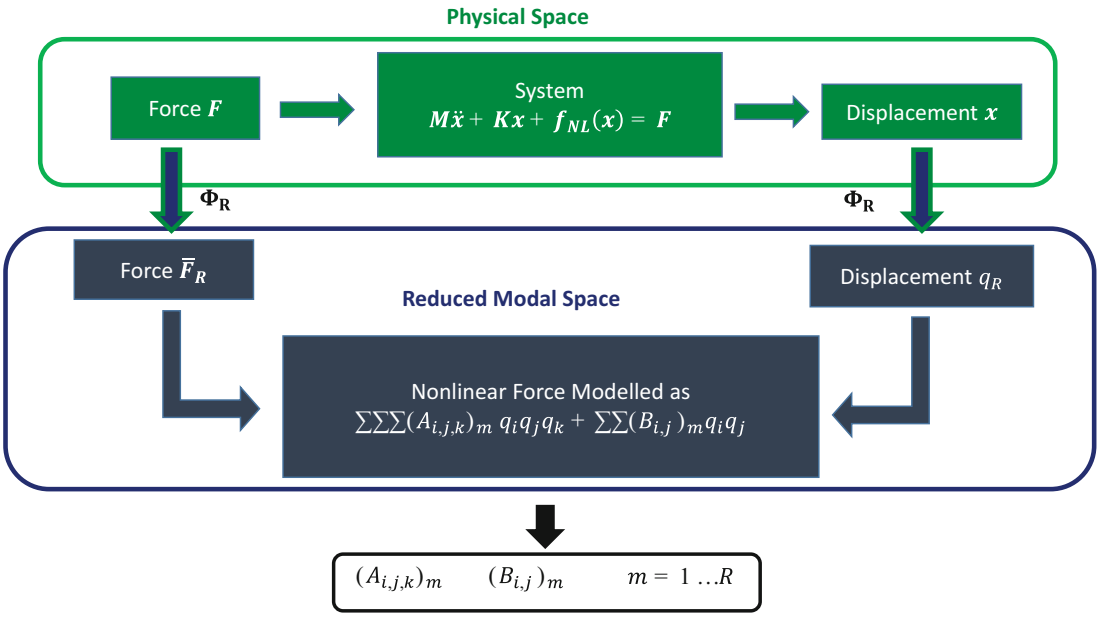

(a) Applied Modal Force Technique

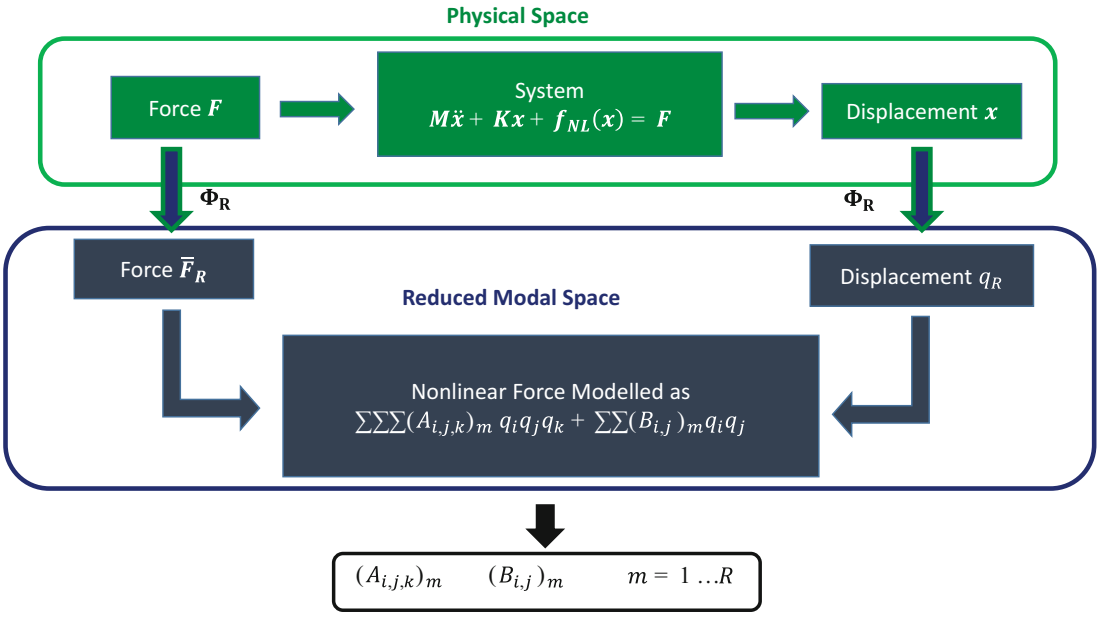

(b) Enforced Modal Displacement Technique

Fig. 36.1 Flow chart describing how the coefficients adopted in the assumed expression for the nonlinear terms in the reduced order model are obtained. Two techniques are presented. (**a**) Applied Modal Force technique. (**b**) Enforced Modal Displacement technique

Then, additional modes can be added using the AMF (EMD) if some components of the reconstructed modal displacement (modal forces) has some 'importance' compared to the components related to the retained modes. The 'importance' is weighted fixing some tolerances. For the sake of clarity, the steps required for finding additional modes to be included is here shown both for the AMF (Eq. 36.5) and the EMD (Eq. 36.6) methods. The physical static response ($\{x^*\}$ and $\{F^*\}$ for the AMF – Eq. 36.5 and EMD – Eq. 36.6) is first obtained using the initial set of modes ($\{q^*\}_T$), then it is projected in the modal space and inspection of the components is possible. Having fixed a tolerance Tol_m, the mode k could be included if $|\{q^*\}_k| > \min(|\{q^*\}_T|) \cdot Tol_m$ or $|\overline{F}_k^*| > \min(|\left\{\overline{F}^*\right\}_R|) \cdot Tol_m$ having adopted the AMF or the EMD method, respectively.

$$\{q^*\} = [\Phi]^{-1}\{x^*\} = [\Phi]^T[M]\{x^*\} \tag{36.5}$$

$$\left\{\overline{F}^*\right\} = [\Phi]\{F^*\} \tag{36.6}$$

The process has been automatized considering as stopping criteria the total number of allowable retained modes; modes are retained until the maximum allowable number is reached.

36.2.3 Coefficient Identification

The last issue that needs to be dealt with is the definition of the static analysis to be run in order to obtain the responses to be used for the identification of the coefficients A_{ijk} and B_{ij}. The key point in the selection is to find out the way of exciting the nonlinearities of the structure of interest without involving non-physical conditions, i.e. exceeding the breaking limit of the structure. It has been recognised that a close solution for the stated issue is a challenge and, to the best of the authors' knowledge, a solution has not been yet identified. Considering the AMF and the EMD, a referential thickness of the structure of interest (t_R) is considered and the set of input force or displacement are consequently defined. In particular, the adopted formula for a single physical input (force – Eq. 36.7 or displacement – Eq. 36.8) are

$$\{F\}_p = [M][\Phi]_T\{C\}_p \tag{36.7}$$

$$\{x\}_p = [\Phi]_T\{C\}_p \tag{36.8}$$

Where

- the sub-index p is varying from 1 to the total number of considered input set. The number of input set needs to be at least equal to the number of unknown coefficients. However, as it is well know in regression analysis, the number of training points needs to be large enough to capture the behaviour of interest whilst avoiding overfitting [26]. Having assumed the nonlinear terms to be expressed as shown in Eq. 36.3, the dimension of the input set has been here fixed to the same one adopted by Hollkhamp et al. [5, 25, 27], i.e.

$$2n + 2(n!/((n-2)!) + 4/3(n!/(n-3)!) \tag{36.9}$$

  This number is automatically obtained following the definition of the scale factor $\{C\}_p$, which follows. It is always greater than the number of unknown coefficients per mode and this is enough to determine the values of the coefficients because the input set is projected in the modal space, thus the dimension of each modal input set is equal to Eq. 36.9.
- $\{C\}_p$ is a column vector of considered scale factor and has the size equal to the number of retained modes. The values of the components are selected in a specific way. The kth component refers to one specific of the retained mode since, in determining the input set (Eqs. 36.7 and 36.8), $\{C\}_p$ multiplies the truncated matrix of eigenvector $[\Phi]_T$. The basic value $C_{p,k}$ is given as follows

$$C_{p,k} = \begin{cases} t_R/\max_{disp}(|\Phi_k|)\cdot\omega_k^2 & \text{if AMF} \\ t_R/\max_{disp}(|\Phi_k|) & \text{if EMD} \end{cases} \tag{36.10}$$

  where $[\Phi]_k$ and ω_k are the eigenvector and the linear frequency (rad/s) related to the kth retained mode. $\max_{disp}$ states for the maximum value among the generalized coordinates that are displacements.

  Both positive and negative values of the stated scale factor are considered. Single or combinations of modal shapes are considered to define the input set, a maximum of 3 modal shapes are considered [5, 25, 27]. Using the expressions for $\{C\}_{p,k}$ previously introduced, this can be accomplished giving values different from zero to three of the total number of components of $\{C\}_p$. Moreover, the coefficients $C_{p,k}$ need to be divided by the number of modes considered in the combination to define the pth input set.

  For the sake of clarity, three examples of scale vectors $\{C\}_p$ considering the AMF technique are here shown. A total of five modes are retained.

1st set C_1 only the second mode is selected, $C_1 = [0, C_{1,2}, 0, 0, 0]'$
2nd set C_2 the second and fourth mode are selected, $C_2 = [0, C_{2,2}, 0, C_{2,4}, 0]' \cdot 1/2$
3rd set C_3 the second, third and fifth mode are selected $C_3 = [0, C_{3,2}, C_{3,3}, 0, C_{3,5}]' \cdot 1/3$

Having defined the input set, the coefficients can be determined adopting the least square methods and additional constraints due to energy considerations [5, 25, 27].

The literature shows that the set of referential thickness (t_R) adopted is often not the one that gives accurate reduced order model [14], thus scale factors need to be adopted to modify the referential thickness. It is important to notice at this point that changing the scale factors, the results are different and this is due to two different reasons if the AMF or the EMF are adopted:

AMF the modes are differently excited since different is the value of the scale factors
EMD the assumption in terms of the nonlinear terms is not correct and thus also the EMD is exciting differently the modes depending on the adopted scale factor

Moreover, if very high frequency modes are adopted, then the input set can acquire excessively large values in some components if the AMF is used (as it is apparent looking at Eq. 36.10), and this has not been previously discussed to the best of the authors' knowledge.

In the method presented here, a strategy is adopted to define the scale factor avoiding excessively large values for the input force if the AMF is adopted and reaching the desired maximum displacement. The stated strategy consists of three main steps:

1. given the modes to be retained a starting input set is defined as shown in Eq. 36.10
2. just for the AMF. Among the modes of interest, defined the low frequency mode of interest; the input set are divided into the set related to low frequency modes and high frequency modes, these are here labelled as $\{IS_{low}\}$ and $\{IS_{high}\}$. Then divide the components of the input set related to forces from those linked to moments ($\{IS_{low/high_F}\}$, $\{IS_{low/high_M}\}$. Reduce by a scale factor S_f the input set $\{IS_{high_F}\}$ and $\{IS_{high_M}\}$ until all the components are less than the maximum component assumed by the input set $\{IS_{low_F}\}$ and $\{IS_{low_M}\}$, respectively.
3. the last step is conceived in order to be sure that the excitation is actually reaching the maximum desired amplitude in the displacement response. This can be accomplished by comparing the actual response and the predicted maximum static linear modal displacement, which is obtained once the input set has been defined ($[\Phi]_T \{C\}_p$). If the static nonlinear response is less (greater) than the predicted linear modal displacement then the input set need to be increased (on decreased). This last step must be done iteratively until the static nonlinear response is within the allowed tolerance $\pm Tol_m$. The adopted method to update the input set is using the following scale factor $V_f(k)$ at the kth iteration

$$V_f(k) = \begin{cases} V_f(k-1)/S & \text{ifi} == 1 \\ |(V_f(k-1) - |V_f(k-1) - V_{f_{store}}(i)|/S)| & \text{otherwise} \end{cases} \tag{36.11}$$

$$V_f(k) = \begin{cases} V_f(k-1)S & \text{ifi} == 1 \\ |(V_f(k-1) + |V_f(k-1) - V_{f_{store}}(i)|/S)| & \text{otherwise} \end{cases} \tag{36.12}$$

where i is the index counting the input set that gives a convergent solution in Abaqus.

The flow chart in Fig. 36.2 summarizes the steps characterizing the developed code in Matlab for the identification of reduced order models. The mode selection, coefficient identification and iterative strategies previously introduced are part of the steps presented in Fig. 36.2. The code can be used to perform iterative analyses if an iterative variation of parametric values or system configuration is of interest. In fact, the main input for the method (in the circular shape box) is the desired configuration for the system. The code is able to update the input file required by the FEM software in order to fulfil the requirement of the user.

36.3 Test Case

The developed strategy presented in Sect. 36.2 is applied here to a crossed beam structure. The structure reproduce a physical system present in our lab and has been modelled in Abaqus (Fig. 36.3 and has 405 nodes and 404 B31 elements).

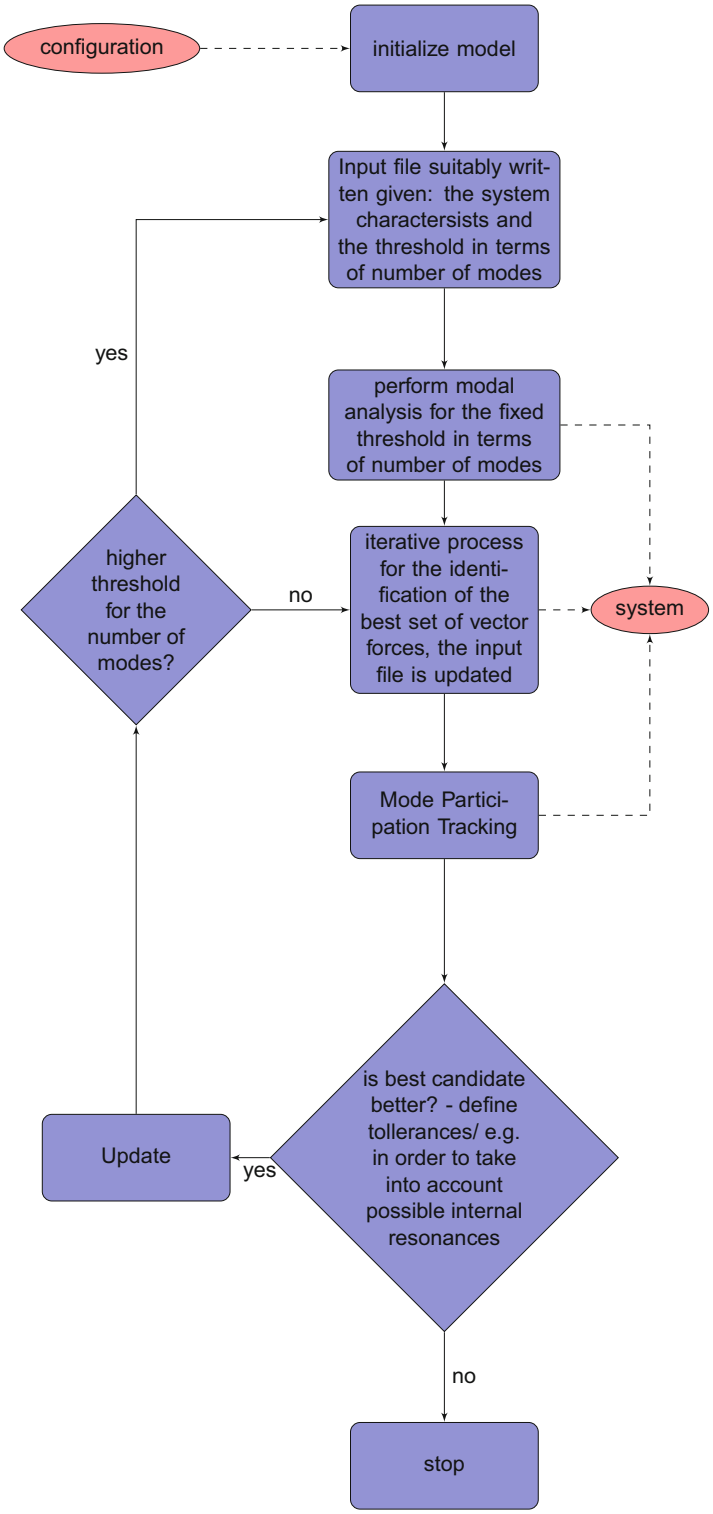

Fig. 36.2 Flow chart of the developed strategies coded in Matlab

Looking at Fig. 36.3, it is apparent that there are three beams, two crossing. The reason for the small crossing beam is purely due to reproduce the physical system, whose has a small crossing beam used for applying forces, as closely as possible. Moreover, along the main crossing beam there are masses that can be moved along the span and this is made possible in

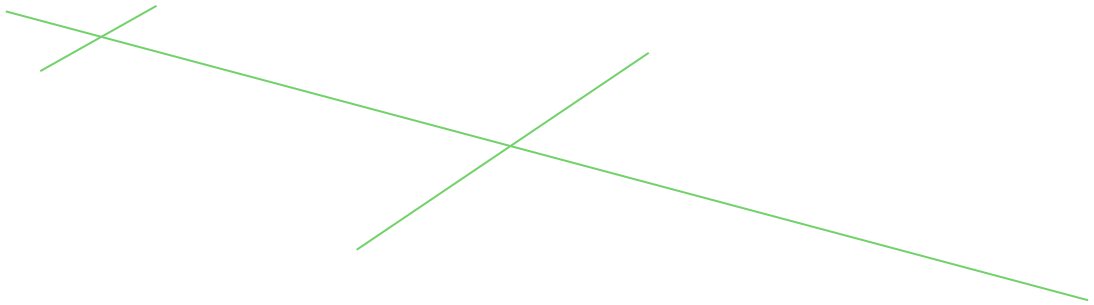

Fig. 36.3 Crossed beam structure modelled in Abaqus

Table 36.1 Elements and properties featuring the crossed beam system

Part	*Number of elements*
Main beam	247
Main crossed beam	102
Secondary crossed beam	43
Masses – main crossed beam	12
Part	*Total length*
Main beam	1 m
Main crossed beam	0.44 m
Secondary crossed beam	0.097 m
Masses – main crossed beam	0.164 m
Part	*Crossed section, dimensions*
Main beam	Rectangular, (0.0127, 0.0064) m
Main crossed beam	Circular, 0.00595 m
Secondary crossed beam	Rectangular, (0.015, 0.015) m
Masses – main crossed beam	Circular, 0.01995 m
Part	*Material*
Main beam	Steel
Main crossed beam	Steel
Secondary crossed beam	Steel
Masses – main crossed beam	Steel

Abaqus by changing the element nodes. Table 36.1 summarizes the number of elements and properties featuring each part of the modelled crossed beam. Regarding the crossed section, the dimensions are referred to the sides or to the diameter if the crossed section is rectangular or circular, respectively.

The features of the steel material are a density equal to 7850 $\mathrm{kg/m^3}$, an Elastic modulus equal to $2.1 \cdot 10^{11}$ Pa and a poisson ratio of 0.3.

Regarding the border conditions, the ends of the main beam allows a translation in the x direction and are supported by two axial springs whose stiffness is $1.85 \cdot 10^6$ kg m.

Finally, there are two further points that need to be covered:

- the position of the crossing beams with respect to the main beam: the main and secondary crossing beam are crossing the main beam at 0.164 and 0.097 m starting from the end more near to the secondary small crossing beam.
- the position of the masses along the main crossed beam: the set of masses is distributed on both the side of the main crossing beam, six on each side and the user can decide where to position them. In what it follows, the six mass elements are next to each other and are moved simultaneously. We will refer to the node of the first of the six set elements to identify the position of the set at each side of the crossing beam. Figures 36.4 and 36.5 in Sect. 36.4 show the crossed beam model created in Matlab, the masses are the red points along the crossed beam.

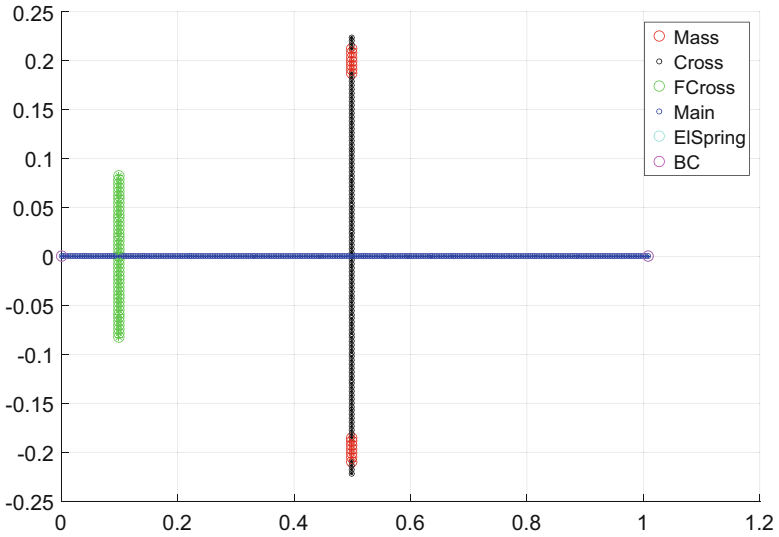

Fig. 36.4 Example of a symmetric configuration

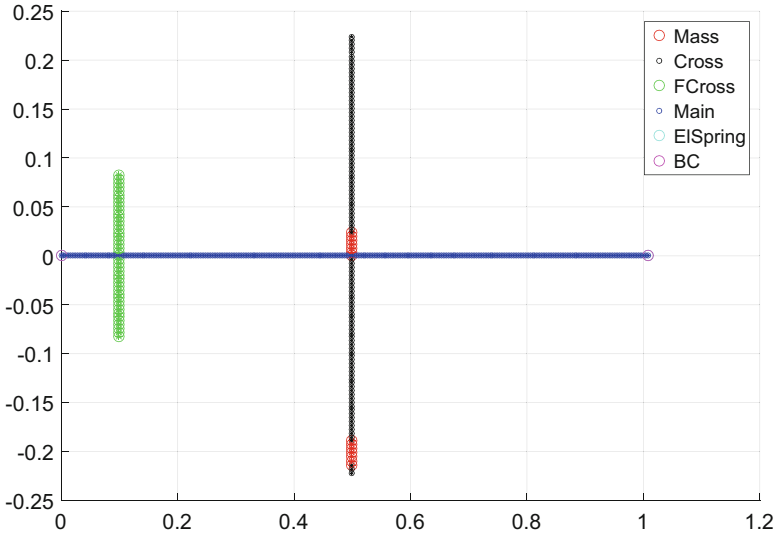

Fig. 36.5 Example of asymmetric configuration having fixed the position on one side at the 49th elements counting from the main beam structure

36.4 Results

The results presented here, cover the investigation of the effect of parametric variation on the linear and nonlinear behaviour of the crossed beam introduced in Sect. 36.3. To such end, linear modal frequencies and nonlinear normal modes [19–21] are considered. These have been obtained using the reduced order models determined following the strategy discussed in Sect. 36.2 and using the COCO software[1] for performing numerical continuation. Before showing and discussing the results, the values for the constant factors adopted in the strategy are here given (Table 36.2).

[1]COCO, https://sourceforge.net/p/cocotools/wiki/Home/, date accessed October, 2016.

Table 36.2 Values adopted for constants featuring the strategy adopted for reduced order modelling under parameter variation

Constant	Value
Tol_f	0.5
t_R	0.05
S_f	1.5
S	2

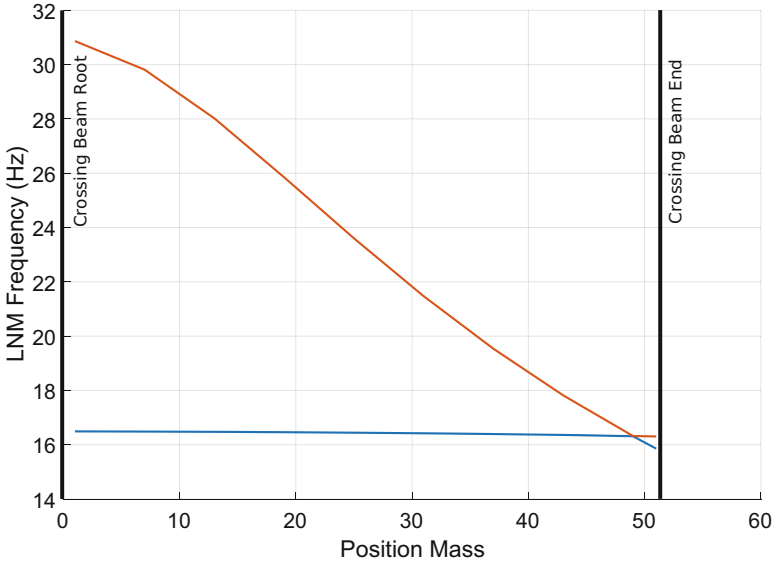

Fig. 36.6 Variation of linear modal frequency if the position of the additional masses is varied symmetrically

The analysis that has been performed and is presented here considers a symmetric and asymmetric parametric variation in terms of the mass elements along the main crossing beam. In particular, the following cases are shown and discussed.

Case a 2 modes are retained, the mass elements are varied symmetrically from the root of the main crossing beam until the end – Fig. 36.4

Case b 2 modes are retained, the mass elements are varied asymmetrically, the set of the masses is kept at a fixed position on one side of the crossing beam – Fig. 36.5

36.4.1 Case a

Having retained the first two modes, the first parametric variation considered is symmetric. In particular, the set of masses is varied symmetrically in both the side of the crossed beam. The strategy presented in Sect. 36.2 has given the possibility of analysing the main effects of the stated parametric variation on linear and nonlinear behaviour. Figure 36.6 shows the variation of the linear modal frequency of the two retained modes as the set of six masses is moved symmetrically along the main crossing beam from the main beam towards the end.

Looking at Fig. 36.6, it is apparent that the two linear frequencies converge as the set of masses approach the 49th position. In particular, the first -lower frequency (second – higher frequency) have a flexional (torsional) modal shape until the position 49 is reached, then a switch in the modal shape occurs.

For each symmetrical configuration, the strategy discussed in Sect. 36.2 is adopted to identify the coefficients characterizing the nonlinear terms and the reduced order models. Figures 36.7 and 36.8 show the first and second NNMs projected in the first and second mode respectively. Different positions for the set of masses are considered and are specified in the legend of the figures. Since the configuration is symmetric, there are neither modal interactions or internal resonances; the amplitude of the first (second) modal coordinate is dominant considering the first (second) NNM. Moreover, as could have been expected from the variation of the linear modal frequencies (Fig. 36.6), the NNMs present a change of variation when the set of masses reaches the position 49. The first NNM presents a slight increment (decrease) in amplitude (frequency) just before the position 49 is reached. Reaching the position 49 the amplitude of the first NNM is suddenly increasing and after the stated position the increment (decrease) in amplitude (frequency) is much more apparent. Similar consideration can be

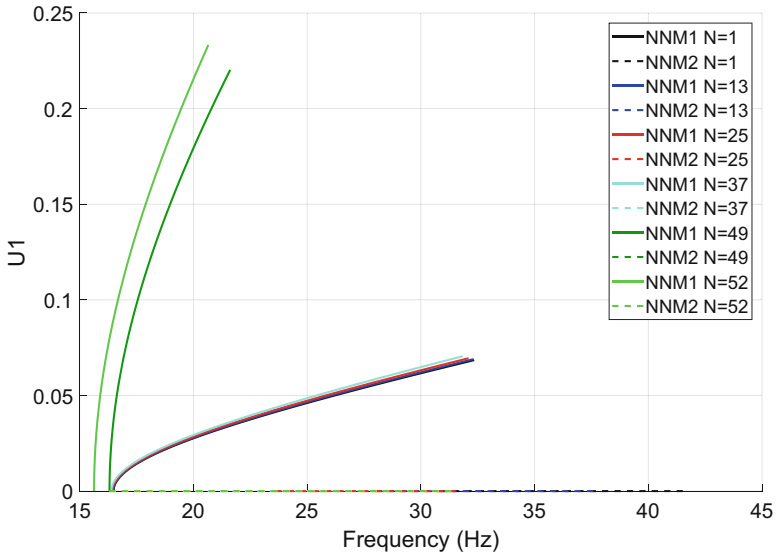

Fig. 36.7 Nonlinear normal modes projected in the first mode obtained retaining the first two modes adopting the AMF for a set of symmetric configuration. The set of masses start at *N* position – defined in the legend – counted starting from the main beam

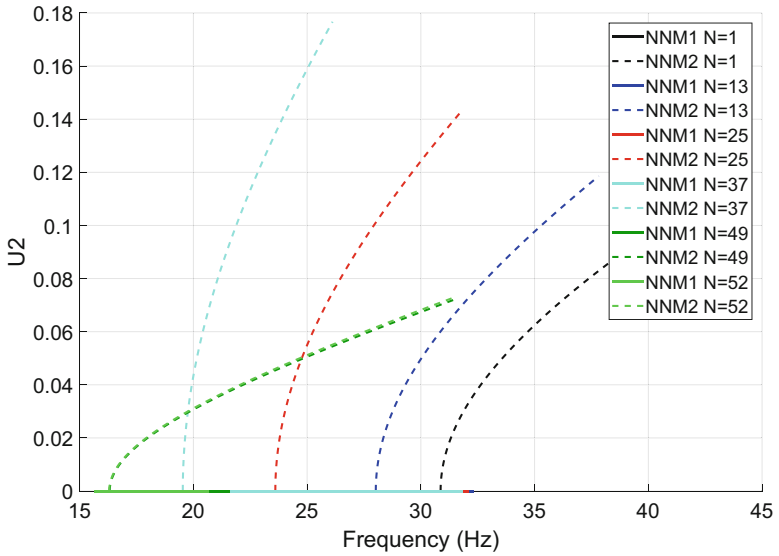

Fig. 36.8 Nonlinear Normal Modes projected in the first mode obtained retaining the first two modes adopting the AMF for a set of symmetric configuration. The set of masses start at *N* position – defined in the legend – counted starting from the main beam

done for the second NNM, the amplitude (frequency) is apparently increasing (decreasing) until the position 49 is reached. At such a position a sudden decrease in amplitude occurs and after such a position, the amplitude and frequency do not change significantly. The stated inversion of behaviour is linked to the change of modal shape of the normal mode. The first (second) mode presents a switch of modal behaviour; from being predominantly flexional (torsional) becomes predominantly torsional (flexional).

36.4.2 Case b

As for the symmetric case, the first two modes have been considered and effects of the asymmetric stated parametric variation on linear and nonlinear behaviour have been investigated looking at nonlinear normal modes. The set of masses is varied asymmetrically changing the position of the masses just on one side of the crossed beam. Figures 36.9 and 36.10 shows the

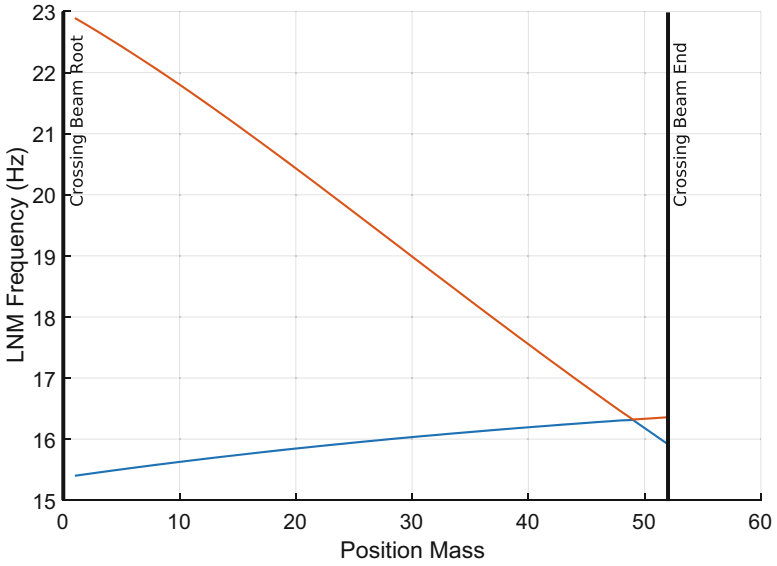

Fig. 36.9 Variation of linear modal frequency if the position of the additional masses is varied asymmetrically, keeping one set of masses fixed at the 49th position on one side

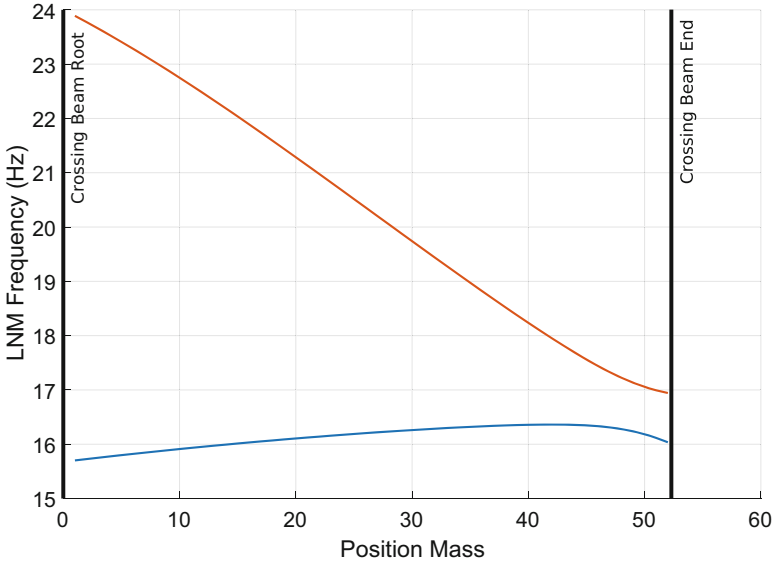

Fig. 36.10 Variation of linear modal frequency if the position of the additional masses is varied asymmetrically, keeping one set of masses fixed at the 43th position on one side

variation of the linear modal frequency of the two retained modes having fixed the set of masses on one side of the main crossing beam at the 49th (Fig. 36.9) and 43th (Fig. 36.10) position.

Looking at Fig. 36.9, and comparing with Fig. 36.6, it is possible to conclude that the considered asymmetry affects the linear frequencies making them closer, thus a possible modal interaction is expected. Moreover, there is a significantly higher decrease in the frequency of the second mode, when predominantly torsional, and a slight higher decrease in the frequency of the first mode, when predominantly flexional.

It is of interest noting that if the fixed position on one side of the main crossing beam is not the 49 the frequencies keep a larger difference between each other. For instance, this is shown in Fig. 36.10 where the linear modal frequencies are obtained having fixed one set of masses at the position 43 along the crossing beam.

As done for the symmetric configuration, NNMs are obtained after having determined the reduced order models. Figures 36.11 and 36.12 show the NNMS projected in the first and second modal coordinate, respectively. Different asymmetric configurations have been considered, having fixed the set of masses at the position 49 on one side of the

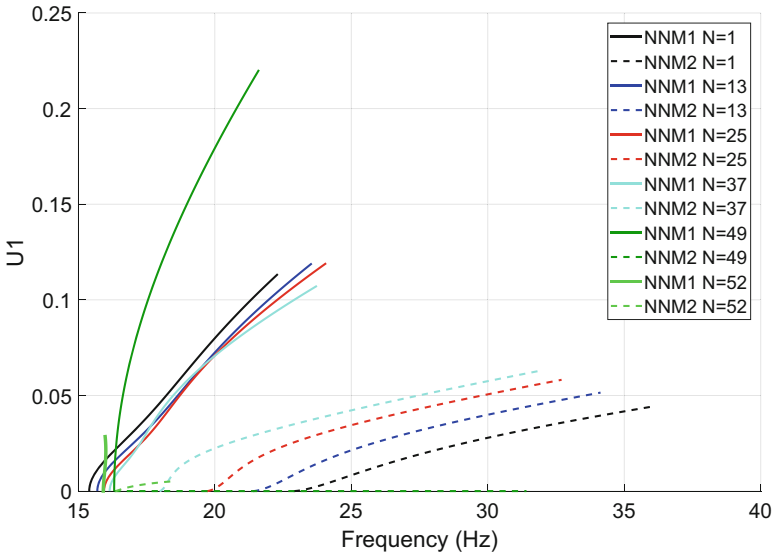

Fig. 36.11 Nonlinear normal modes projected in the first mode retaining the first two modes adopting the AMF for a set of asymmetric configuration. On one side of the crossed beam the set of masses is fixes at the 49th position. On the other side the set of masses starts at the *N* position – defined in the legend – counted starting from the main beam

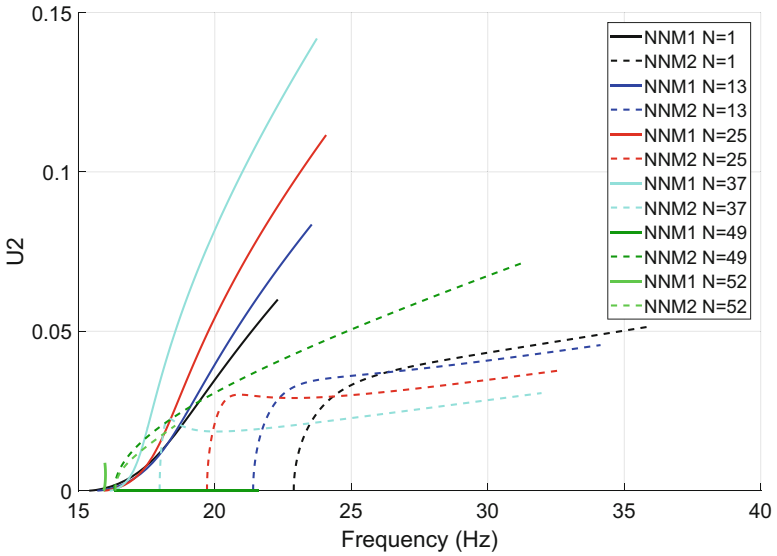

Fig. 36.12 Nonlinear normal modes projected in the second mode retaining the first two modes adopting the AMF for a set of asymmetric configuration. On one side of the crossed beam the set of masses is fixes at the 49th position. On the other side the set of masses starts at the *N* position – defined in the legend – counted starting from the main beam

crossing beam. The position of the set of masses on the other side of the crossing beam is specified in the legend of each figure. A different behaviour is shown if compared to the NNMs obtained for the symmetric configuration. The asymmetry causes modal interaction and this is apparent looking at the NNMs projected both in the first and second modal coordinate; the amplitude of the second (first) modal coordinate have a significant amplitude if compared to the first (second) modal coordinate for the first (second) NNM. Moreover, for each modal coordinate, at a fixed frequency, the amplitude of the two NNMs are very close to each other.

Finally the occurrence of modal interactions for all asymmetric configurations has been checked looking at the modal shape. This can be shown investigating the ratio between the first and the second (second and first) modal coordinate for the second (first) NNM. Figures 36.13 and 36.14 show the stated ratio for the first and second NNM, respectively. The ratio is plotted as the frequency changes and for the different asymmetric configurations adopted for testing the code and identifying the reduced order model. As for the NNM, the position of the 'moving' set of masses is specified in the legend. Moving

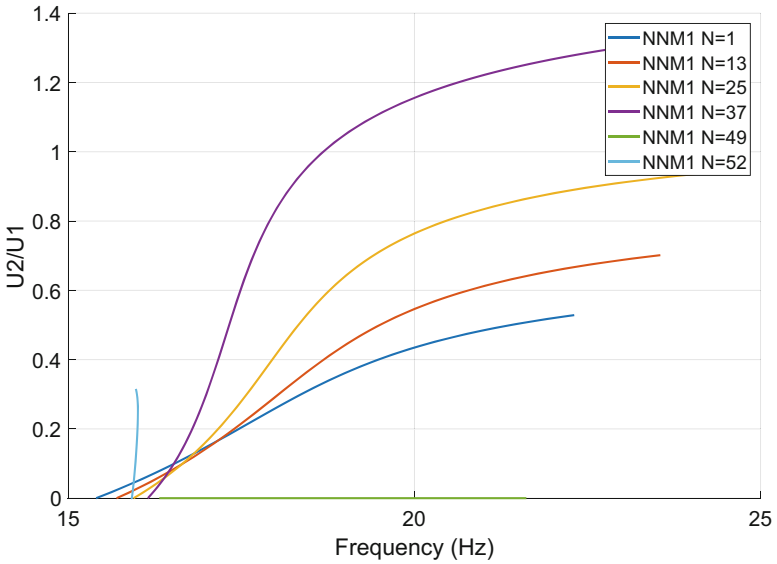

Fig. 36.13 Amplitude of the second mode over the first one along the first backbone curves

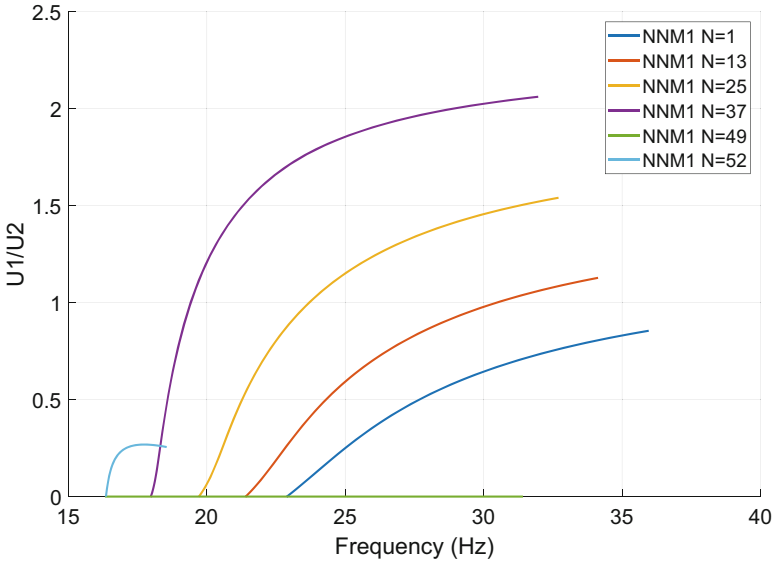

Fig. 36.14 Amplitude of the first mode over the second one along the second backbone curves

the set of masses along the main crossing beam, from the main beam until the position 49 (at which the set of masses on the other side of the crossing beam is fixed) the modal interaction increases. When the position 49 is reached, the modal interaction disappears and is slightly present again moving further than the position 49. Note that if the ratio between the modal coordinates is greater than 1 it means that the second (first) mode is prevalent in the modal shape of the first (second) NNM.

36.5 Conclusions

A strategy for performing nonlinear modal reduction using either the applied modal force (AMF) or the enforced modal displacement (EMD) has been presented. The technique is conceived with the aim of using it in an automatic environment. It has been implemented in a Matlab environment and allows the automatic exchange of information with the FEM software,

Abaqus. The conceived strategy allows the investigation of the effects of parametric variation on linear and nonlinear behaviour of the system of interest. The validation considers a crossed beam structure modelled in Abaqus and the presented results have been obtained using the AMF technique. Symmetric and asymmetric configurations have been investigated. The results reveal that modal interaction occurs only in the presence of asymmetric configurations and disappears when the systems is in a symmetric configuration. These results are encouraging and the potential for such an automatic environment for modal reduction in the presence of parameter variation is powerful. Further investigation needs to be done in terms of the assumptions made for the description of the nonlinear terms, i.e. considering only quadratic and cubic terms, and of the modal participation. Moreover, comparison with the results obtained using the EMD technique and validation of the identified nonlinear normal modes will be covered in the future steps of our research.

References

1. McEwan, M.I., Wright, J.R., Cooper, J.E., Leung, A.Y.T.: A combined modal/finite element analysis technique for the dynamic response of a non-linear beam to harmonic excitation. J. Sound Vib. **243**(4), 601–624 (2001)
2. Detroux, T., Renson, L., Masset, L., Kerschen, G.: The harmonic balance method for bifurcation analysis of large-scale nonlinear mechanical systems. Comput. Methods Appl. Mech. Eng. **296**, 18–38 (2015)
3. Przekop, A., Guo, X., Rizzi, S.A.: Alternative modal basis selection procedures for reduced-order nonlinear random response simulation. J. Sound Vib. **313**, 4005–4024 (2012)
4. Kuether, R.J., Allen, M.S.: Validation of nonlinear reduced order models with time integration targeted at nonlinear normal modes. Nonlinear Dyn. **1**, 363–375 (2016)
5. Kuether, R.J., Allen, M.S., Hollkhamp, J.J.: Modal substructuring of geometrically nonlinear finite-element models. AIAA J. **54**(2), 691–702 (2016)
6. Kuether, R.J., Allen, M.S., Hollkhamp, J.J.: Modal substructuring of geometrically nonlinear finite element models with interface reduction. AIAA J. **55**(5), 1695–1706 (2017)
7. VanDamme, C.I., Allen, M.S.: Using NNMs to evaluate reduced order models of curved beam. In: De Clerck, J., Epp, D.S. (eds.) Rotating Machinery, Hybrid Test Methods, Vibro-Acoustics & Laser Vibrometry, vol. 8, pp. 457–469. Springer International Publishing, Cham (2016)
8. Spottswood, S.M., Allemang, R.J.: Identifying nonlinear parameters for reduced order models. Part I: an analytical comparison. In: IMAC-XXIV: Conference & Exposition on Structural Dynamics (2006)
9. Fujimoto, K., Scherpen, J.M.A.: Balanced realization and model order reduction for nonlinear systems based on singular value analysis, SIAM J. Control Optim. **48**(7), 4591–4623 (2010)
10. Rizzi, S.A., Przekop, A.: The effect of basis selection on static and random acoustic response prediction using a nonlinear modal simulation. J. Sound Vib. **313**, 4005–4024 (2012)
11. Rizzi, S.A., Przekop, A.: System identification-guided basis selection for reduced-order nonlinear response analysis. J. Sound Vib. **315**, 467–485 (2008)
12. VanDamme, C.I., Allen, M.S.: Evaluating NLROMs' ability to predict dynamic snap through of a curved beam in a random loading environment. In: 58th AIAA/ASCE/AHS/ASC Structures, Structural Dynamics, and Materials Conference, Grapevine, 9–13 Jan 2017
13. Guerin, L.C.M., Kuether, R.J., Allen, M.S.: Considerations for indirect parameter estimation in nonlinear reduced order models. Nonlinear Dyn. **1**, 327–342 (2016)
14. Kuether, R.J., Deaner, B.J., Hollkhamp, J.J., Allen, M.S.: Evaluation of geometrically nonlinear reduced-order models with nonlinear normal modes. AIAA J. **53**(11), 3273–3285 (2015)
15. Kuether, R.J., Brake, M.R., Allen, M.S.: Evaluating convergence of reduced order models using nonlinear normal modes. Model Valid. Uncertain. Quantif. **3**, 287–300 (2014)
16. Allen, M.S., Kuether, R.J., Deaner, B.J., Sracic, M.W.: A numerical continuation method to compute nonlinear normal modes using modal reduction. In: 53rd AIAA/ASME/ASCE/AHS/ASC Structures, Structural Dynamics and Materials Conference, Honolulu (2012)
17. Chang, Y.-W., Wang, X., Capiez-Lernout, E., Mignolet, M.P., Soize, C.: Reduced order modelling for the nonlinear geometric response of some curved structures. In: AAAF-AIAA. International Forum on Aeroelasticity and Structural Dynamics, Paper IFASD-2011-185, Paris, pp. 1–19, June 2011
18. Gordon, R.W., Hollkamp, J.J.: Reduced-order models for acoustic response prediction, Final report (2011)
19. Serandour, G., Peeters, M., Kerschen, G., Golinval, J.C.: Computation of nonlinear normal modes, part II: numerical continuation in AUTO. In: ENOC-2008, Saint Petersburg (2008)
20. Hill, T.L., Neild, S.A., Cammarano, A.: An analytical approach for detecting isolated periodic solution branches in weakly nonlinear structures. J. Sound Vib. **379**, 150–165 (2016)
21. Hill, T.L., Neild, S.A., Cammarano, A., Wagg, D.J.: An analytical approach for detecting isolated periodic solution branches in weakly nonlinear structures. J. Sound Vib. **379**, 135–149 (2016)
22. Noël, J., Detroux, T., Masset, L., Kerschen, G., Virgin, L.: Isolated response curves in a base-excited, two-degree-of-freedom, nonlinear system. In: Proceedings of the ASME 2015 International Design Engineering Technical Conferences & Computers and Information in Engineering Conference, Boston (2015)

23. Kuether, R., Renson, L., Detroux, T., Grappasonni, C., Kerschen, G., Allen, M.: Nonlinear normal modes, modal interactions and isolated resonance curves. J. Sound Vib. **351**, 299–310 (2015)
24. Detroux, T., Habib, G., Masset, L., Kerschen, G.: Performance, robustness and sensitivity analysis of the nonlinear tuned vibration absorber. Mech. Syst. Signal Process. **60–61**, 799–809 (2015)
25. Hollkamp, J.J., Gordon, R.W., Spottswood, S.M.: Nonlinear modal models for sonic fatigue response prediction: a comparison of methods. J. Sound Vib. **284**, 1145–1163 (2005)
26. Forrester, A., Sbester, A., Keane, A.: Engineering Design via Surrogate Modelling: A Practical Guide. Wiley, Chichester (2008)
27. Hollkamp, J.J., Gordon, R.W.: Reduced-order models for nonlinear response prediction: implicit condensation and expansion. J. Sound Vib. **318**, 1139–1153 (2008)